Relationships between geometries and energies of identity S_N2 transition states: the dominant role of the distortion energy and its origin

DAVID JOHN MITCHELL
DuPont Canada Research Centre, P.O. Box 5000, Kingston, Ont., Canada K7L 5A5

H. BERNHARD SCHLEGEL
Department of Chemistry, Wayne State University, Detroit, MI 48202, U.S.A.

SASON S. SHAIK[1]
Laboratoire de Chimie Théorique, Bâtiment 490, Université de Paris-Sud, 91405, Orsay, France

AND

SAUL WOLFE[2]
Department of Chemistry, Queen's University, Kingston, Ont., Canada K7L 3N6

Received September 13, 1984

This paper is dedicated to Professor Camille Sandorfy on the occasion of his 65th birthday

DAVID JOHN MITCHELL, H. BERNHARD SCHLEGEL, SASON S. SHAIK, and SAUL WOLFE. Can. J. Chem. **63**, 1642 (1985).

At the 4-31G computational level, the intrinsic barriers of eight identity S_N2 reactions $X^- + CH_3X \rightarrow XCH_3 + X^-$ are less than the energies required to distort CH_3X from its ground state geometry to its transition state geometry by a constant 25 kcal/mol. The distortion energy and its C—X stretching and H—C—X bending components can be calculated directly, or, alternatively, estimated from the force constants and bond dissociation energies of CH_3X. Regardless of the mode of computation, the distortion energies are found to be dominated by the C—X stretching deformations, and these are linearly correlated with the intrinsic barriers. The total deformation energies are also linearly correlated with the intrinsic barriers. The transition vectors of the eight identity reactions have been calculated; each is dominated by the C—X stretch. The percentage of C—X stretching at the transition state, here termed the Distortion Index (DI), reflects the "tightness" or "looseness" of this structure. The intrinsic barrier increases as the DI increases, i.e., as the transition state becomes more "exploded". This result does not agree with the predictions of a More O'Ferrall – Jencks potential energy surface diagram. However, as shown in some detail, all of the computational results of the present work are in harmony with the surface crossing diagram model of the barrier. The essential feature of this model is the notion that the activation process in an identity S_N2 reaction is a result of the distortion that is required to transfer one electron from X^- to CH_3X.

DAVID JOHN MITCHELL, H. BERNHARD SCHLEGEL, SASON S. SHAIK et SAUL WOLFE. Can. J. Chem. **63**, 1642 (1985).

Des calculs au niveau 4-31G indiquent que les énergies des barrières intrinsèques de 8 réactions S_N2 d'identité: $X^- + CH_3X \rightarrow XCH_3 + X^-$ sont systématiquement 25 kcal/mol de moins que celles requises pour déformer le CH_3X de sa géométrie de l'état fondamental jusqu'à celle de l'état de transition. L'énergie de déformation, ainsi que ses composantes d'élongation C—X et de déformation H—C—X peuvent être calculées directement, ou évaluées, à partir des constantes de force et des énergies de dissociation des liaisons du CH_3X. Peu importe le mode de calcul, on a trouvé que les énergies de dissociation sont dominées par les déformations de l'élongation du C—X et celles-ci peuvent être reliées linéairement aux barrières intrinsèques. Les énergies de déformation totale sont également reliées linéairement aux barrières intrinsèques. On a calculé les vecteurs de transition des 8 réactions d'identité; chacune est dominée par l'élongation de C—X. Le pourcentage d'élongation de C—X au niveau de l'état de transition, que l'on appelle ici l'indice de distortion (ID), reflète la nature compacte ou lâche de cette structure. La barrière intrinsèque augmente avec l'ID, c'est-à-dire au fur et à mesure que l'on s'éloigne de l'état de transition. Ce résultat ne s'accorde pas avec les prédictions d'un diagramme de surface d'énergie potentielle de More O'Ferrall – Jencks. Cependant, tel que montré avec certains détails, tous les résultats obtenus par le calcul sont en accord avec le modèle de diagramme de croisement de surface de la barrière. La caractéristique essentielle de ce modèle réside dans le fait que le processus d'activation dans une réaction S_N2 est un résultat de la distorsion qui est requise pour transférer un électron de X^- à CH_3X.

[Traduit par le journal]

Introduction

The course of an S_N2 reaction $Y^- + CH_3X \rightarrow YCH_3 + X^-$ is attended by a number of changes in molecular geometry. A deformation of the H—C—H angles occurs as the configuration about the carbon atom is inverted, the C—X bond stretches and is broken, and the C—Y bond shortens and is formed. The changes in geometry are accompanied by changes in the total energy of the system. For a gas phase reaction, the nature of the latter has been discussed extensively (1, 2), and the reaction coordinate has been found to have the form shown in Fig. 1. In Fig. 1, $Y^- \ldots CH_3X$ and $YCH_3 \ldots X^-$ are reactant and product ion–molecule complexes (clusters), and $(Y—CH_3—X)^-$ is the S_N2 transition structure.

In an earlier communication (3), it was observed that linear relationships exist between stretching and bending geometrical parameters of $(Y—CH_3—X)^-$ transition structures and the thermochemistry of non-identity S_N2 reactions. One objective of the present work is to study the relationships between calculated geometrical parameters of identity S_N2 transition structures (Y = X) and the calculated barriers ($\Delta E_0^{\neq}$) associated with such reactions (see Fig. 2). A second objective is to demonstrate that the Surface Crossing Diagram (SCD) model (4–6), which ascribes the origin of the S_N2 barrier to the energy required to transfer *one* electron from X^- to CH_3X, accounts for

[1] Permanent address: Department of Chemistry, Ben Gurion University, Beer Sheva 84105, Israel.

[2] Author to whom correspondence may be addressed.

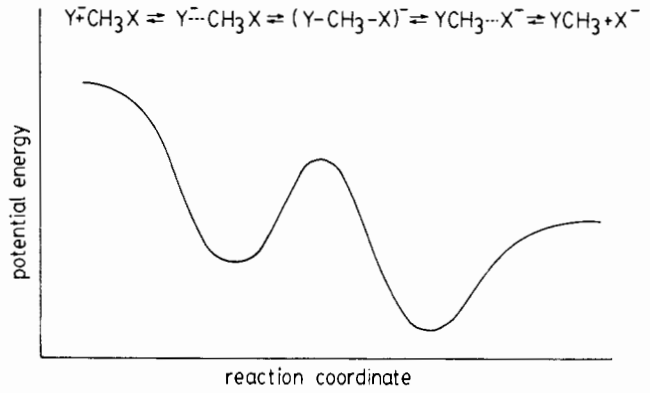

FIG. 1. Reaction coordinate for a non-identity S_N2 reaction $Y^- + CH_3X \rightarrow YCH_3 + X^-$.

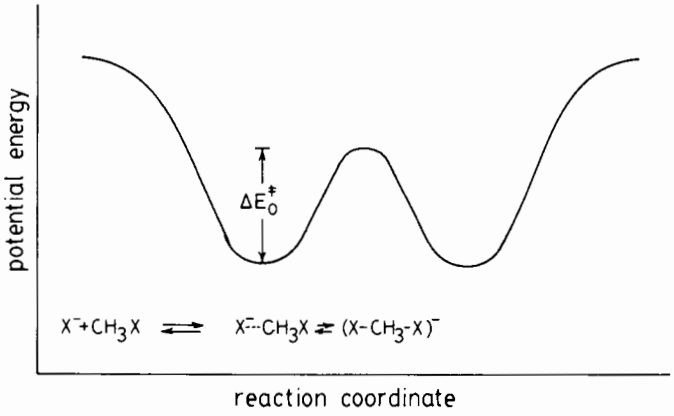

FIG. 2. Reaction coordinate for an identity S_N2 reaction $X^- + CH_3X \rightarrow XCH_3 + X^-$. The intrinsic barrier $\Delta E_0^{\ddagger}$ is given by the energy difference between the ion–molecule cluster $X^- \ldots CH_3X$ and the transition structure $(X{-}CH_3{-}X)^-$.

all of the results.

For the reaction coordinate of Fig. 2, the region from cluster to cluster is of greatest interest, since it encompasses most of the geometrical changes. Because the fully optimized geometries and energies of $X^- \ldots CH_3X$ clusters and $(X{-}CH_3{-}X)^-$ transition structures were already available from HF/4-31G computations for X = H, HCC, NC, CN, HO, HS, F, Cl (2, 3, 7), a detailed examination of the relationships between these quantities was performed at this level. Additional computations were performed, as needed, using the 4-31G basis set and the GAUSSIAN 80 (8) or GAUSSIAN 82 (9) programmes.

Computational results

Table 1 summarizes the primary data: $\Delta E_0^{\ddagger}$ is the intrinsic barrier, R_1 is the C—X bond length of CH_3X in the cluster, R_2 is the C—X bond length in the transition structure, f_R is the calculated CH_3—X stretching force constant, f_θ is the calculated bending force constant for the umbrella deformation of the methyl group, and $f_{R\theta}$ is the stretch–bend interaction force constant.

The intrinsic barrier can be partitioned (10) into the energy required to deform the CH_3X moiety, and the interaction energy between X^- and the deformed CH_3X. An approximate estimate of the deformation energy can be obtained from the calculated force constants of CH_3X. To change CH_3X from its geometry in the cluster to its geometry in the transition state requires

TABLE 1. Calculated intrinsic barriers, force constants, and C—X bond lengths for gas phase S_N2 reactions[a]

X	$\Delta E_0^{\ddagger}$[b]	R_1 (Å)[c]	R_2 (Å)[d]	f_R (au)[e]	f_θ (au)[f]	$f_{R\theta}$ (au)[g]
H	52.0	1.089	1.730	0.378	0.926	0.068
CCH	50.4	1.465	2.124	0.387	1.059	0.144
*C*N	43.8	1.459	2.112	0.380	1.062	0.148
*N*C	28.5	1.441	2.013	0.407	1.133	0.207
OH	21.2	1.463	1.908	0.367	1.009	0.199
SH	15.6	1.914	2.459	0.195	0.846	0.138
F	11.7	1.462	1.828	0.450	1.142	0.213
Cl	5.5	1.965	2.382	0.285	1.033	0.192

[a] HF/4-31G calculations.
[b] In kcal/mol.
[c] Refers to C—X bond length in CH_3X having the geometry of the cluster.
[d] Refers to C—X bond length in CH_3X having the geometry of the transition state.
[e] Units are hartree $bohr^{-2}$; 1 hartree = 627.51 kcal/mol; 1 bohr = 0.529 Å.
[f] Units are hartree rad^{-2}.
[g] Units are hartree $rad^{-1}\ bohr^{-1}$.

TABLE 2. Intrinsic barriers, approximate deformation energies, and the components of these deformation energies,[a] for reactions $X^- + CH_3X \rightarrow XCH_3 + X^-$

X	D_{C-X}	ΔE_R^{approx}	ΔE_θ^{approx}	$\Delta E_{R\theta}^{approx}$	ΔE_{def}^{approx}	$\Delta E_0^{\ddagger}$
H	104	55.0	33.6	−17.7	70.9	52.0
CCH	117	60.5	44.2	−41.1	63.6	50.4
*C*N	114	58.6	41.8	−40.6	59.8	43.8
*N*C	90[b]	47.2	42.8	−48.8	41.2	28.5
OH	91	34.1	34.8	−34.8	34.1	21.2
SH	73	27.2	28.3	−29.1	26.4	15.6
F	108	32.3	36.6	−29.5	39.4	11.7
Cl	84	26.0	28.5	−28.5	26.3	5.5

[a] All energies are in kcal/mol.
[b] Estimated from D_{CH_3-CN} (114 kcal/mol) and $-\Delta H$ for the isomerization of CH_3NC to CH_3CN (23.7 kcal/mol) (12).

a stretch of the C—X bond by ΔR, and a bend of the H—C—X angle by $\Delta\theta$, as well as smaller changes in the rest of the molecule. Since stretching potentials are very anharmonic, it is not possible to estimate the energy associated with a C—X stretch from harmonic force constants alone. Therefore, to approximate the stretching anharmonicity, a Morse curve (11) was fitted to the calculated harmonic stretching force constant, f_R, and the experimental C—X bond dissociation energies, D, using eq. [1], where $\Delta R = R_2 - R_1$.

$$[1] \quad \Delta E_R^{approx} = D[1 - \exp(-\beta\Delta R)]^2; \quad \beta = (f_R/2D)^{1/2}$$

The data are shown in Table 2, and Fig. 3 is a plot of ΔE_R^{approx} versus $\Delta E_0^{\ddagger}$. The two quantities are linearly related (r = 0.975).

The energy required to bend an H—C—X angle can be estimated directly from the calculated harmonic force constant f_θ (eq. [2]), because the bond anharmonicity is small.

$$[2] \quad \Delta E_\theta^{approx} = \tfrac{1}{2} f_\theta (\Delta\theta)^2$$

The stretch–bend interaction must also be taken into account, because bending of the H—C—X angles is greatly facilitated by the stretch of the C—X bond. In the harmonic approximation, the stretch–bend interaction is given by eq. [3].

$$[3] \quad \Delta E_{R\theta}^{approx} = f_{R\theta}(\Delta R)\ (\Delta\theta)$$

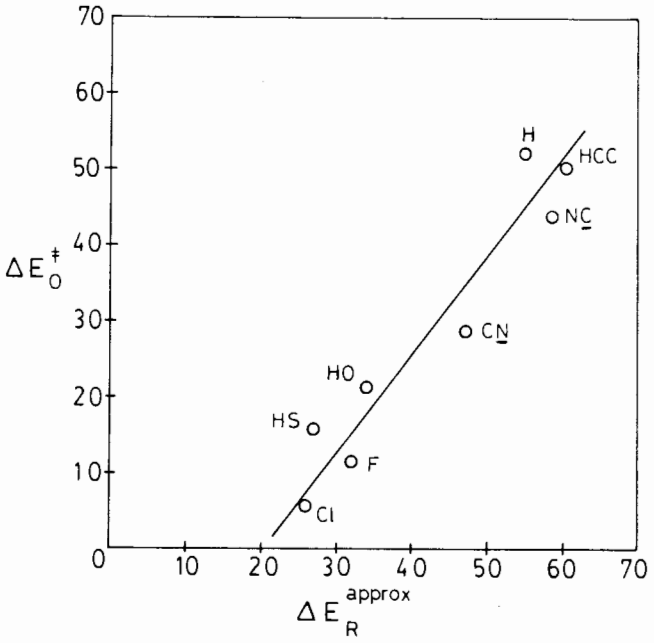

FIG. 3. A plot of ΔE_R^{approx} versus $\Delta E_0^{\ddagger}$ for eight identity S_N2 reactions. Energies are in kcal/mol.

In terms of the approximations of eqs. [1]–[3], the total deformation energy is given by eq. [4]. All of these quantities are included in Table 2.

$$[4] \quad \Delta E_{def}^{approx} = \Delta E_R^{approx} + \Delta E_\theta^{approx} + \Delta E_{R\theta}^{approx}$$

The deformation energies just described are approximations, because they are based on the calculated force constants and experimental dissociation energies of CH_3X. The actual deformation energies, ΔE_{def}, and their components can be calculated directly, as shown in Scheme 1. The stretching deformation energy, ΔE_R, is obtained from the energy difference between **3** and **1**, where **1** refers to CH_3X in the geometry of the cluster, and **3** is derived from **1** by a stretch of the C—X bond to its value in the transition structure **2**. The bending deformation energy, ΔE_θ, is obtained analogously from the energy difference between **1** and **4**, where **4** refers to bending of **1** to the bond angles of the transition structure. The total deformation energy is the energy difference between **1** and **2**. The quantities ΔE_{def}, ΔE_R, and ΔE_θ are collected in Table 3.[3]

Figures 4, 5, and 6 show, respectively, plots of ΔE_R, ΔE_θ, and ΔE_{def} versus $\Delta E_0^{\ddagger}$. The relationship between ΔE_R and $\Delta E_0^{\ddagger}$ is linear ($r = 0.954$), as is the relationship between ΔE_{def} and $\Delta E_0^{\ddagger}$ ($r = 0.979$), but ΔE_θ is poorly correlated with $\Delta E_0^{\ddagger}$. In addition, inspection of the data of Table 3 reveals that ΔE_{def} is dominated by the stretching deformation.

The most interesting observation is that the quantity ($\Delta E_{def} - \Delta E_0^{\ddagger}$) is constant. For this series of eight X's, at the HF/4-31G level, the difference is 25.1 ± 3.3 kcal/mol. *This is an important result. It implies that the differences in the intrinsic barriers result from the differences in* ΔE_{def}*; the effect of the anion* X^- *is approximately constant.* As will be discussed below, this finding, especially, constitutes strong support for the State Correlation Diagram (SCD) model of the S_N2 barrier.

[3] For X = F, the ΔE_{def} calculated from the energy difference between **1** and **2** is the same as the deformation energy obtained from a Morokuma analysis (10). The authors thank Dr. J. M. Lefour (Orsay) for checking this point.

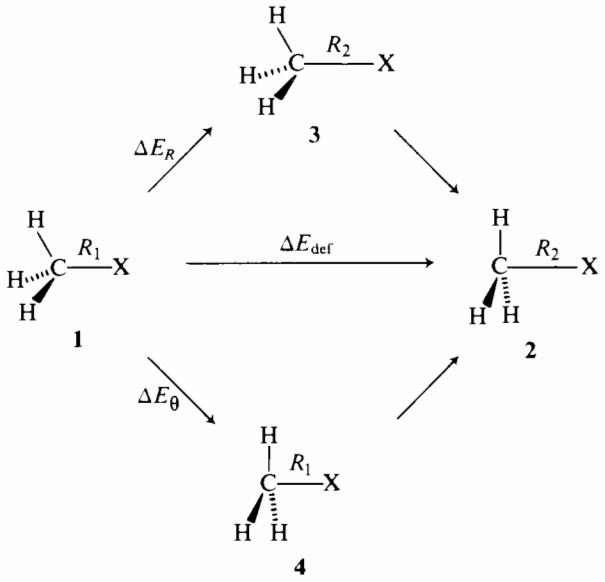

SCHEME 1

TABLE 3. Calculated deformation energies and the components of these deformation energies[a] for reactions $X^- + CH_3X \rightarrow XCH_3 + X$

X	ΔE_R	ΔE_θ	ΔE_{def}	$\Delta E_0^{\ddagger}$	$(\Delta E_{def} - \Delta E_0^{\ddagger})$
H	67.4	28.6	71.7	52.0	19.7
CCH	74.7	39.5	73.5	50.4	23.1
*C*N	68.7	36.0	67.0	43.8	23.2
*N*C	63.1	38.3	57.0	28.5	28.5
OH	45.7	45.9	52.1	21.2	30.9
SH	37.2	28.7	38.8	15.6	23.2
F	38.8	30.4	40.8	11.7	29.1
Cl	27.6	18.5	28.9	5.5	23.4

[a] In kcal/mol.

As an additional probe of the identity S_N2 surface near the top of the barrier, vibrational frequency calculations were carried out for the eight transition states. Each structure has one imaginary frequency whose magnitude depends on the mass of X and on the curvature of the surface. The normal coordinate that corresponds to the imaginary frequency is the transition vector, which points along the intrinsic reaction path linking reactants and products. The transition vectors for the eight identity reactions are summarized in Table 4. To facilitate comparisons, in Fig. 7 the vectors have been shifted by an overall translation, to allow the central carbon atoms to remain stationary.

All of the transition vectors are very similar, despite the differences in the intrinsic barriers, and are dominated in each case by a C—X stretch. There is also a component of bend. Analysis of the force constants of the transition structures reveals that the bending potential has a positive curvature, and the stretching potential has a small positive or negative curvature; the stretch–bend interaction is always negative, and accounts for a sizeable fraction of the negative curvature. This analysis therefore indicates that the C—X stretch dominates the energetics associated with the barrier process, but the intrinsic reaction path requires the concerted action of stretching and bending at the transition state.

The foregoing computational results may be summarized as follows.

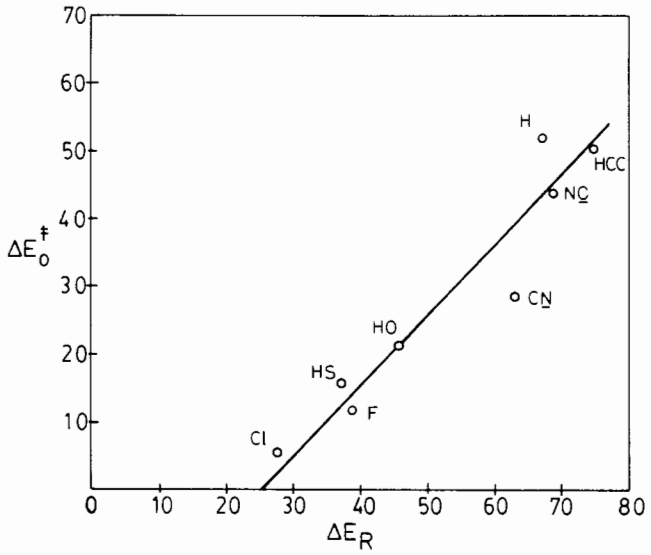

FIG. 4. A plot of ΔE_R versus $\Delta E_0^{\ddagger}$ for eight identity S_N2 reactions. Energies are in kcal/mol.

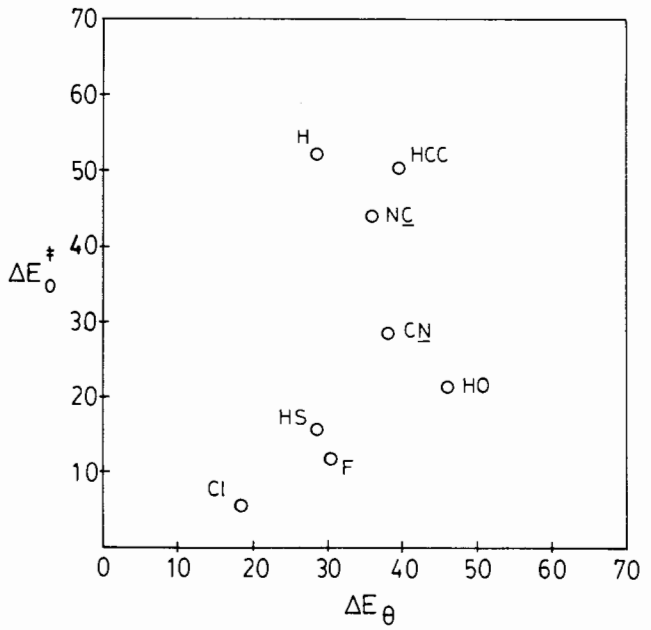

FIG. 5. A plot of ΔE_θ versus $\Delta E_0^{\ddagger}$ for eight identity S_N2 reactions. Energies are in kcal/mol

(a) The activation process of an identity S_N2 reaction is dominated by the deformation energy required to bring CH_3X from its geometry in the cluster to its geometry in the transition state.

(b) The deformation energy depends on the nature of X, and follows the order H $\simeq$ HCC $\simeq$ *C*N > *N*C > HO > HS > F > Cl.

(c) The C—X stretch is the distinguished deformation leading to the transition state.

(d) The C—X stretch required to achieve the transition state is linearly correlated with the intrinsic barrier.

Interpretation of the results in terms of the SCD model of the S_N2 barrier

An understanding of the activation process in the S_N2 reaction requires an understanding of the results just described. In the SCD model, the correlation diagram appropriate to an identity S_N2 reaction is shown in Fig. 8 (5*a*, *b*), whose anchor points are the two ground states and the two charge transfer states of the clusters. The transition state results from an avoided crossing of the two curves, and its geometry coincides with the crossing point.

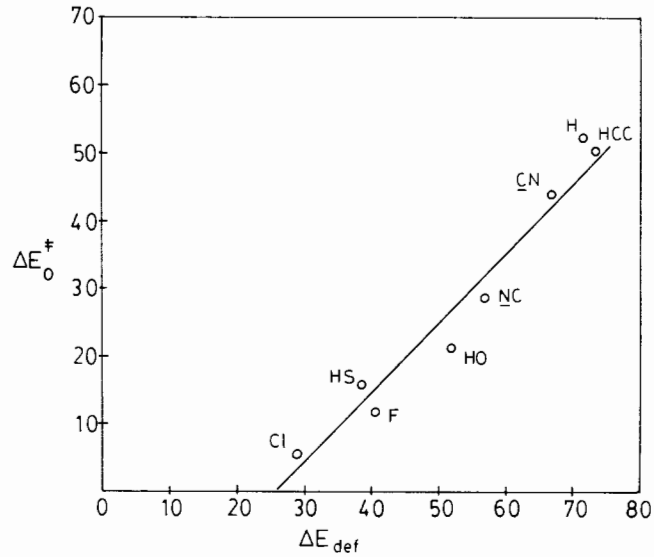

FIG. 6. A plot of ΔE_{def} versus $\Delta E_0^{\ddagger}$ for eight identity S_N2 reactions. Energies are in kcal/mol.

TABLE 4. X—CH_3—X transition vectors in internal coordinates

X	ΔR (C—X)[a]	$\Delta\theta$ (CH—C—X)[b]
H	0.797	0.206
HCC	1.012	0.506
*C*N	1.115	0.481
*N*C	1.125	0.461
HO	1.014	0.480
HS	1.122	0.492
F	1.120	0.531
Cl	1.128	0.439

[a] In atomic units.
[b] In radians.

At this point, the ground state $X^{\cdot-}R—X$ and the charge transfer state $X\cdot(R—X)^{-}$ have the same energy. Because of the energy gap that separates the two states at the beginning of the reaction, the crossing that achieves the transition state must be driven by molecular distortions (5, 13). The effects of these distortions are a destabilization of the ground state, and a concomitant stabilization of the charge transfer state.

That the ground state should be destabilized by the distortions depicted in **5** is self-evident. The charge transfer state is stabilized by the transformation of the $(R—X)^{-}$ radical anion bond into a covalent X—R bond on the opposite side of R.

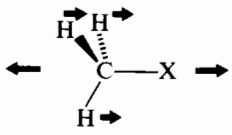

5

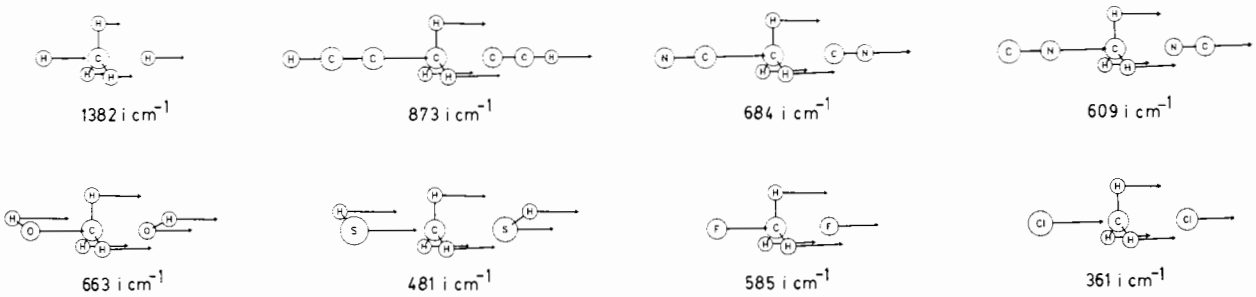

FIG. 7. Transition vectors for eight identity S_N2 transition structures. Calculations performed at the HF/4-31G level using GAUSSIAN 82.

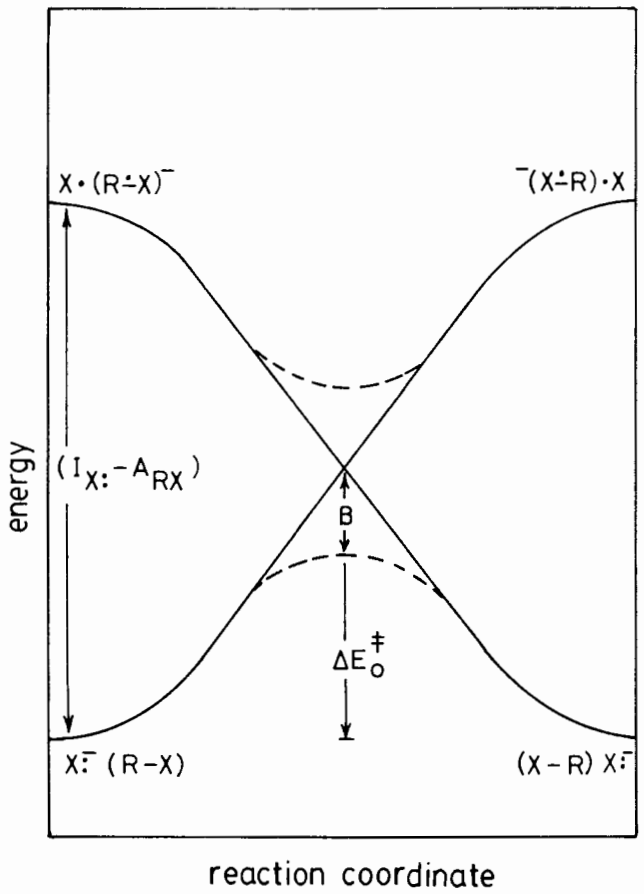

FIG. 8. State correlation diagram for the identity S_N2 reaction. The minima along the reaction coordinate refer to the ion–molecule clusters, and the maxima refer to the charge transfer states. The avoided crossing is given by B, $\Delta E_0^{\ddagger}$ is the central barrier, and (I_X - A_{RX}) is the electron transfer energy gap. The reaction coordinate can be defined as the difference between the X . . . R and R . . . X distances.

The conclusion that the S_N2 barrier results from the distortion required to reach the crossing point of the ground and charge transfer states provides a physical model for the correlation between $\Delta E_0^{\ddagger}$ and ΔE_{def}. In addition, two features of Fig. 8 allow the magnitudes of $\Delta E_0^{\ddagger}$ and ΔE_{def} to be estimated. One is the electron transfer energy gap (eq. [5]) that has to be overcome by the molecular distortions, where $I_{X:}$ is the ionization potential of X^- and A_{RX} is the electron affinity of RX. The second is the curvature of the functions that connect the ground and charge transfer states. When the distortion is inefficient, a shallow descent of the charge transfer state will be observed, as shown in Fig. 9A. An efficient distortion will lead to a steep descent from the charge transfer state, as shown in Fig. 9B. For X's characterized by the same gap, the S_N2 barrier will decrease as the distortion becomes more efficient. As discussed elsewhere (5*a*, *b*, *d*, 6), the steepness or shallowness of descent in such cases is determined by the degree of delocalization of the odd electron in the radical anion $(R\dot{-}X)^-$. For example, delocalization in the radical anion results in a shallow descent for two reasons: (1) the distortion must overcome the delocalization energy; (2) the delocalization inhibits bond coupling between X· and $(R\dot{-}X)^-$.

[5] $\quad \text{gap} = I_{X:} - A_{RX}$

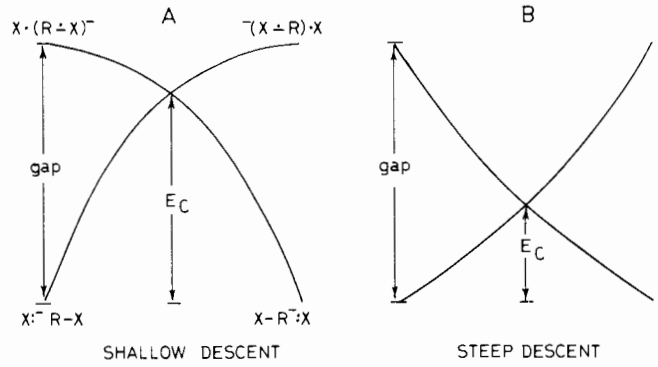

FIG. 9. (A) Shallow descent from the charge transfer state, a property of delocalized radical anions $(R\dot{-}X)^-$. (B) Steep descent from the charge transfer state, corresponding to efficient distortion of the charge transfer state.

A radical anion may possess two modes of delocalization, termed intralinkage and interlinkage. The intralinkage mode is defined by eq. [6], where $W_{R:}$ and $W_{X:}$ refer to the weights (i.e., the squares of the coefficients) of the resonance forms $R:^-\cdot X$ and $R\cdot:X^-$, respectively.

[6] $\quad (R\dot{-}X)^- = W_{R:}(R:^-\cdot X) + W_{X:}(R\cdot:X^-); \quad W_{R:} + W_{X:} = 1$

In a delocalized radical anion, $W_{R:}$ is large. This delocalizes the odd electron on X of $(R\dot{-}X)^-$ and leads to the inhibition of bond coupling noted above.

The interlinkage mode occurs whenever R bears two or more identical leaving groups X, as in CH_2Cl_2 or CH_4. In such cases the odd electron will be delocalized over all identical linkages (5*d*) as depicted in eq. [7] for $(CH_4)^{\dot{-}}$, where N is the normalization constant.

[7] $\quad (CH_4)^{\dot{-}} = N[H\dot{-}\underset{H}{\overset{H}{C}}-H + H-\underset{H}{\overset{H}{C}}\dot{-}H + \ldots\ldots]$

Since the odd electron may also exhibit intralinkage de-

localization in the sense of eq. [6], such radical anions will be strongly delocalized; S_N2 reactions in these cases will be characterized by the shallow descent depicted in Fig. 9A.

The total index of delocalization $\bar{W}_{R:}$ can be taken as the product of the intralinkage index $W_{R:}$ and the interlinkage index. The latter is given by the inverse of the normalization constant of eq. [7], which takes into account the number of bonds that participate in delocalization. For example, in $(CH_4)^{\cdot}$ the interlinkage index is $(4)^{-1/2}$.

$$[8] \quad \bar{W}_{R:} = W_{R:}/N$$

The deformation energy required to reach the transition state can be set approximately equal to the height of the crossing point E_C (Figs. 9A, 9B) above the cluster. As is evident from Figs. 8, 9A, and 9B, E_C is a fraction, f, of the energy gap $(I_{X:} - A_{RX})$, and this fraction is proportional to $W_{R:}$, leading to eq. [9]. A similar expression holds for the barrier itself, with the modification that the avoided crossing B (Fig. 8) must be subtracted from E_C. This leads to eq. [10].

$$[9] \quad \Delta E_{def} \sim E_C = f(I_{X:} - A_{RX}); \quad f \propto \bar{W}_{R:}$$

$$[10] \quad \Delta E_0^{\neq} = f(I_{X:} - A_{RX}) - B; \quad f \propto \bar{W}_{R:}$$

As discussed elsewhere (5, 6, 13), the avoided crossing is approximately constant for the identity reactions (B = 14 kcal/mol) (5*a*, *b*, *d*). This result is thus consistent with the HF/4-31G computational finding that ΔE_{def} differs from $\Delta E_0^{\neq}$ by a constant 25 kcal/mol. Equation [10] can be simplified further and given quantitative predictive ability by setting the proportionality constant between f and $\bar{W}_{R:}$ equal to unity (5) (eq. [11]).

$$[11] \quad \Delta E_0^{\neq} \text{ (kcal/mol)} = \bar{W}_{R:}(I_{X:} - A_{RX}) - 14$$

Equations [9] and [11] reveal that trends in $\Delta E_0^{\neq}$ and in ΔE_{def} will be determined by the interplay between $\bar{W}_{R:}$ and $(I_{X:} - A_{RX})$. This point is illustrated by the data collected in Table 5, viz., the reactivity indices $(I_{X:} - A_{RX})$ and $\bar{W}_{R:}$, the calculated ΔE_{def}, the calculated $\Delta E_0^{\neq}$, and the $\Delta E_0^{\neq}$ given by eq. [11]. The deformation energy is large and the barrier is large when the electron transfer energy gap $(I_{X:} - A_{RX})$ is large, or when the shallowness index $(\bar{W}_{R:})$ is large. For example, in entries 1 and 2, $\bar{W}_{R:}$ is approximately constant; and the reaction $F^- + CH_3F$ has a higher $\Delta E_0^{\neq}$ and a higher ΔE_{def} than the reaction $Cl^- + CH_3Cl$ because the electron transfer energy is larger in the former case. Similarly, in entries 3, 4, and 5, $\bar{W}_{R:}$ is again approximately constant; in these cases as well, $\Delta E_0^{\neq}$ and ΔE_{def} increase as the electron transfer energy gap increases.

On the other hand, comparison of entries 1 and 4, for which the energy gap is approximately constant, shows that $HO^- + CH_3OH$, the reaction having the larger $\bar{W}_{R:}$, has the larger $\Delta E_0^{\neq}$ and the larger ΔE_{def}.

In summary, the Surface Crossing Diagram model (Fig. 8) and its quantitative representation (eq. [11]) reproduce the calculated trends in $\Delta E_0^{\neq}$ and ΔE_{def}. It follows that the activation process in an identity S_N2 reaction is a result of the distortion that is required to transfer one electron from $X:^-$ to CH_3X.

The availability of a physical model of the activation process allows the trends in the transition state geometries to be interpreted. In an identity S_N2 reaction, the distortion that distinguishes one X from another is $\Delta R = (R_2 - R_1)$, the change in the C—X bond length from the cluster to the transition state. The percentage of C—X lengthening at the transition state may be defined as the Distortion Index, DI (eq. [12]). This reflects the "tightness" or "looseness" of the transition state. A large DI corresponds to a looser or "exploded" (14) transition state.

TABLE 5. Reactivity indices, ΔE_{def}, $\Delta E_0^{\neq}$, and $\Delta E_0^{\neq}$ (eq. [11]), for $X^- + CH_3X \rightarrow XCH_3 + X^-$ reactions[a]

Entry	X	$I_{X:} - A_{RX}$[b]	$\bar{W}_{R:}$[b]	ΔE_{def}[c]	$\Delta E_0^{\neq}$	$\Delta E_0^{\neq}$ (eq. [11])[c]
1	Cl	113	0.251	28.9	5.5	14.4
2	F	135	0.242	40.8	11.7	18.7
3	HS	95	0.340	38.8	15.6	18.1
4	HO	109	0.357	52.1	21.2	24.9
5	HCC	145	0.362	73.5	50.4	38.5
6	NC	159	0.309	67.0	43.8	34.5
7	H	84	0.720	71.7	52.0	46.5

[a] In kcal/mol.
[b] See refs. 5*a*, *b*, *d*, and 6.
[c] Present work.

$$[12] \quad \text{DI} = 100\Delta R/R_1$$

The factors that control the DI are, again $(I_{X:} - A_{RX})$ and $\bar{W}_{R:}$. The first defines the energy gap that must be overcome by the distortion. The second reflects the ability of the distortion to decrease the energy of the charge transfer state. The following trends are predicted.

(a) For a series of reactions $X^- + CH_3X$ in which the degree of radical anion delocalization $(\bar{W}_{R:})$ remains constant, DI will increase as the energy gap increases, i.e., the transition state will become looser.

(b) For a series of $X^- + CH_3X$ reactions in which the energy gap remains constant, DI will increase as $\bar{W}_{R:}$ increases.

The data of Table 6 illustrate these points. From entries 1 and 2, which have the same $\bar{W}_{R:}$, it is seen that the looser transition state (larger DI) is obtained for $F^- + CH_3F$, which has the larger charge transfer energy gap. Similarly, in entries 3, 4, and 5, the looseness of the transition state again increases as the energy gap increases. On the other hand, entries 1 and 4 demonstrate that, for a constant gap, the transition state becomes looser as $\bar{W}_{R:}$ increases. Clearly, delocalization of the radical anion (larger $\bar{W}_{R:}$) leads to a loosening of the transition structure. The loosest transition state is thus observed for $H^- + CH_4$, because this leads to the most delocalized radical anion.

Table 6 also illustrates an additional correlation, between $\Delta E_0^{\neq}$ and the Distortion Index. The tightest transition state ($Cl^- + CH_3Cl$) has the lowest barrier, and the loosest transition state ($H^- + CH_4$) has the highest barrier.

What has thus emerged is a direct link between deformation energies, barriers, and transition state geometries, each of which is a consequence of the activation process in an S_N2 reaction. This unified insight has resulted from the notion that the activation process is itself a result of the distortion required to transfer a single electron from $X:^-$ to X across the CH_3 moiety of CH_3X.

The foregoing analysis of the trends in transition state geometries should be contrasted with the predictions of potential energy surface diagrams (PESD) (cf. Fig. 10) (15). For an identity S_N2 reaction the four corners of the PESD model represent reactants, products, the triple ion configuration $(X^- + CH_3^+ + X^-)$, and the high energy hypervalent structure $(XCH_3X)^-$. The transition state lies at the midpoint between reactants and products, and changes in X can make the transi-

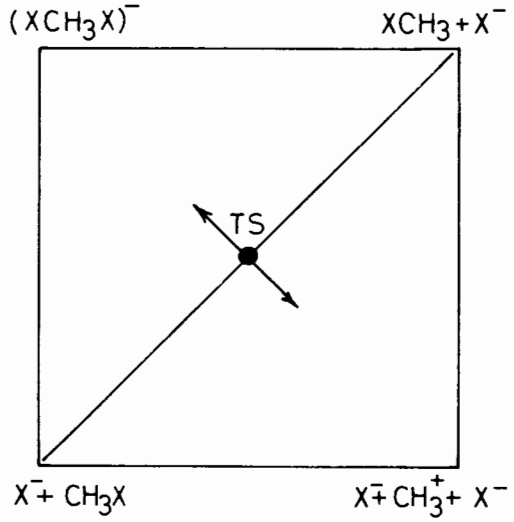

FIG. 10. Potential energy surface diagram for the identity S_N2 reaction.

TABLE 6. Electron transfer energies, radical anion delocalization indices, distortion indices, and intrinsic barriers for $X^- + CH_3X \rightarrow XCH_3 + X^-$ reactions

Entry	X	$I_{X\cdot} - A_{RX}$[a]	$\bar{W}_{R\cdot}$	DI[b]	$\Delta E_0^{\neq}$[a,b]
1	Cl	113	0.251	21.1	5.5
2	F	135	0.242	25.0	11.7
3	HS	95	0.340	28.0	15.6
4	HO	109	0.357	30.4	24.9
5	HCC	145	0.362	45.0	50.4
6	N*C*	159	0.309	44.8	43.8
7	H	84	0.720	58.0	52.0

[a] In kcal/mol.
[b] 4-31G calculations.

tion state tighter or looser, as indicated by the arrows in Fig. 10. Ignoring the effect of the high energy $(XCH_3X)^-$ corner, as is customary, leads to the following conclusion: if a change in X decreases the energy of the triple ion corner, the transition state will shift towards this corner, *and become looser*. For example, replacement of X = H by X = Cl should lead to a looser transition state, because $(Cl^- + CH_3^+ + Cl^-)$ is at least 40 kcal/mol more stable than $(H^- + CH_3^+ + H^-)$.

The trends of Table 5 are just the opposite of this important prediction of the PESD model. It is, therefore, not clear how the PESD model can be employed to rationalize the computational results of the present work.

Acknowledgements

This work was supported by the Natural Sciences and Engineering Research Council of Canada and the National Science Foundation (U.S.A.). One of the authors (S.S.S.) thanks the Laboratoire de Chimie Théorique (Orsay) for support during his sabbatical leave.

1. M. J. PELLERITE and J. I. BRAUMAN. J. Am. Chem. Soc. **105**, 2672 (1983), and references cited therein.
2. D. J. MITCHELL. Ph.D. Thesis. Queen's University, 1981, and references cited therein.
3. S. WOLFE, D. J. MITCHELL, and H. B. SCHLEGEL. J. Am. Chem. Soc. **103**, 7692 (1981).
4. S. S. SHAIK. J. Am. Chem. Soc. **103**, 3692 (1981).
5. (*a*) S. S. SHAIK. Nouv. J. Chim. **6**, 159 (1982); (*b*) S. S. SHAIK and A. PROSS. J. Am. Chem. Soc. **104**, 2708 (1982); (*c*) S. S. SHAIK and A. PROSS. Bull. Soc. Chim. Belg. **91**, 355 (1982); (*d*) S. S. SHAIK. J. Am. Chem. Soc. **105**, 4359 (1983); (*e*) S. S. SHAIK. Nouv. J. Chim. **7**, 201 (1983); (*f*) A. PROSS and S. S. SHAIK. Acc. Chem. Res. **16**, 363 (1983); (*g*) S. S. SHAIK. J. Am. Chem. Soc. **106**, 1227 (1984).
6. S. S. SHAIK. Prog. Phys. Org. Chem. In press.
7. S. WOLFE, D. J. MITCHELL, and H. B. SCHLEGEL. J. Am. Chem. Soc. **103**, 7694 (1981).
8. J. S. BINKLEY, R. A. WHITESIDE, R. KRISHNAN, R. SEEGER, D. J. DEFREES, H. B. SCHLEGEL, S. TOPIOL, L. R. KAHN, and J. A. POPLE. QCPE, **13**, 406 (1981).
9. J. S. BINKLEY, M. J. FRISCH, D. J. DEFREES, K. RAGHAVACHARI, R. A. WHITESIDE, R. SEEGER, H. B. SCHLEGEL, and J. A. POPLE. To be published.
10. S. NAGASE and K. MOROKUMA. J. Am. Chem. Soc. **100**, 1666 (1978).
11. P. M. MORSE. Phys. Rev. **34**, 210 (1932).
12. M. H. BAGHAL-VAYJODEE, J. L. COLLISTER, and H. O. PRITCHARD. Can. J. Chem. **55**, 2634 (1977).
13. S. S. SHAIK. Isr. J. Chem. In press.
14. B. L. KNIER and W. P. JENCKS. J. Am. Chem. Soc. **102**, 6789 (1980).
15. E. R. THORNTON. J. Am. Chem. Soc. **89**, 2915 (1967); R. A. MORE O'FERRALL. J. Chem. Soc. B, 274 (1970); W. P. JENCKS. Chem. Rev. **72**, 705 (1972); J. C. HARRIS and J. L. KURZ. J. Am. Chem. Soc. **92**, 349 (1970); J. E. CRITCHLOW. J. Chem. Soc. Faraday Trans. **68**, 1774 (1972); D. A. JENCKS and W. P. JENCKS. J. Am. Chem. Soc. **99**, 7948 (1977); A. J. KRESGE. Acc. Chem. Res. **8**, 354 (1975).